Interleaved Time-Frequency Multiple Access using OTFS Modulation

Rose Mary Augustine and A. Chockalingam

Department of ECE, Indian Institute of Science, Bangalore 560012

Abstract—In this paper, we consider a multiuser uplink scenario using orthogonal time frequency space (OTFS) modulation and propose a scheme for multiplexing users on an $N \times M$ time-frequency grid in which allocated time-frequency resource blocks for different users are non-contiguous and interleaved. The proposed scheme, termed as *interleaved time-frequency multiple access* (ITFMA), allows multiuser interference-free signal reception in the time-frequency domain thereby reduces the detection complexity. The proposed scheme is shown to achieve improved bit error performance compared to another recently proposed OTFS based multiple access scheme. We also consider the peak-to-average power ratio (PAPR) of the proposed scheme and analytically characterize its complementary cumulative distribution function for large values of N/q, where q denotes the interleaving period in time. The use of DFT precoding is shown to improve the PAPR of the proposed scheme.

Keywords: OTFS modulation, time-frequency domain, delay-Doppler domain, multiple access, PAPR.

I. INTRODUCTION

Orthogonal time frequency space (OTFS) modulation is a two-dimensional (2D) modulation scheme proposed recently to combat the dynamics of rapidly time-varying channels which are doubly dispersive in nature [1]. OTFS modulation embeds the information symbols in the delay-Doppler domain rather than in the time-frequency domain by using transformations which result in a 2D convolutional interaction of the information symbols with the delay-Doppler channel [2],[3]. OTFS modulation has been shown to offer several benefits like superior bit error performance and efficient channel estimation in rapidly time-varying channels compared to conventional multicarrier modulation schemes designed in the time-frequency (TF) plane [2]-[11]. Another key advantage of OTFS is that it can be implemented over any multicarrier modulation scheme using pre- and post processing transformations [7].

In this paper, we consider uplink multiuser communication using OTFS modulation. It has been suggested in [3] that multiplexing users in one OTFS frame can be done in two ways, either in delay-Doppler (DD) domain or in time-frequency (TFF) domain. The former way multiplexes users in the delay-Doppler plane by allocating distinct delay-Doppler resource blocks (DDRBs) to different users [12],[14]. In [12], allocation of contiguous DDRBs to users which results in multiuser interference (MUI) has been proposed. The use of guard bins can help to avoid MUI, but it affects the spectral efficiency. The second multiplexing way is to allocate different time-frequency resource blocks (TFRBs) to different users. This allocation can be done either in contiguous or interleaved fashion. In [13], a multiple access method which multiplexes users in the TF plane in a contiguous way which is MUI-free in the TF domain has been presented. This is achieved

by allotting interleaved DD bins to each user so that the corresponding TF signal can be limited to occupy a contiguous non-overlapping region in the TF plane. We term this scheme as the contiguous time-frequency multiple access (CTFMA) scheme. The TF signal of each user is detected over its localized region using a reduced point inverse OTFS transform. In [14], the bit error performance of the schemes in [12] and [13] in high mobility environments on the uplink have been evaluated and compared with those of other well known multiple access schemes such as OFDMA and SC-FDMA. In [15], a non-orthogonal multiple access (NOMA) scheme for OTFS has been proposed, where high-mobility users are served in the DD plane using OTFS modulation while low-mobility users are served in the TF plane using conventional OFDM.

This paper proposes a novel interleaved way of multiplexing users in the TF plane for OTFS multiple access on the uplink, wherein users are allocated non-overlapping and interleaved TFRBs for transmission. We term the proposed scheme as interleaved time-frequency multiple access (ITFMA) scheme using OTFS modulation. The multiplicative action of the channel with each user's signal in the TF domain ensures that the signals corresponding to each user are separable on the TF plane and can be detected independently at the receiver. We also analyze the peak-to-average power ratio (PAPR) characteristics of the proposed scheme and show that the use of DFT precoding on the proposed scheme results in improved PAPR characteristics. The proposed scheme is shown to achieve better PAPR characteristics and bit error performance compared to the scheme in [13].

The rest of the paper is organized as follows. The system model of the proposed ITFMA scheme is presented in Sec. II. The PAPR analysis of the ITFMA scheme is presented in Sec. III. Bit error rate (BER) and PAPR performance results and discussions are presented in Sec. IV. Conclusions are presented in Sec. V.

II. ITFMA SYSTEM MODEL FOR OTFS BASED UPLINK

Consider an OTFS based multiple access system with K_u uplink users communicating with a base station (BS). Each user is equipped with a single transmit antenna and the BS is equipped with a single receive antenna. Each user employs OTFS modulation architected over a multicarrier modulation scheme. In OTFS, information symbols are embedded in an $N \times M$ delay-Doppler grid denoted by Γ, given by

$$\Gamma = \{(\tfrac{k}{NT}, \tfrac{l}{M\Delta f}), k = 0, \cdots, N-1, l = 0, \cdots, M-1\}, \quad (1)$$

where $1/NT$ and $1/M\Delta f$ denote the Doppler resolution and delay resolution, respectively, and N and M are the number of Doppler and delay bins, respectively. The DD grid is designed

such that $\nu_{\max} < \Delta f < 1/\tau_{\max}$, where $\tau_{\max}$ and $\nu_{\max}$ denote the maximum delay and Doppler spread of the multiuser channel, respectively. Let $x_u[k,l]$, $k = 0, \cdots, N-1$, $l = 0, \cdots, M-1$, and $u = 0, \cdots, K_u - 1$ denote the symbol transmitted by the uth user on the (k,l)th DD grid point/bin. The corresponding time-frequency lattice Λ, reciprocal to Γ is given by

$$\Lambda = \{(nT, m\Delta f), n = 0, \cdots, N-1, m = 0, \cdots, M-1\}. \tag{2}$$

Hence, the signal in the TF domain, denoted by $X_u[n,m]$, $n = 0, \cdots, N-1$, $m = 0, \cdots, M-1$, occupies a duration NT and a bandwidth of $M\Delta f$.

The proposed ITFMA scheme multiplexes the users in the TF lattice Λ non-contiguously in an interleaved fashion such that each user's TF signal occupies only MN/K_u TF bins/resource blocks which are spaced at equal intervals, p bins along the frequency axis and q bins along the time axis. These intervals are chosen such that $K_u = pq$ with $p|M$ (i.e., M is an integer multiple of p) and $q|N$. When $p = 1, q = K_u$, users are interleaved along time and each user can occupy all the frequency resource bins. Similarly, when $p = K_u, q = 1$, users are interleaved along the frequency and each user can span the entire time resource bins. This interleaving pattern can be obtained in the TF plane when in the corresponding delay-Doppler domain each user quasi-periodically repeats (repeats with a multiplicative phase) the MN/K_u information symbols so as to occupy the entire delay-Doppler grid. That is, for $k = 0, \cdots, N-1$, $l = 0, \cdots, M-1$, $k' = 0, \cdots, \frac{N}{q} - 1$, $l' = 0, \cdots, \frac{M}{p} - 1$, $d = 0, \cdots, q-1$, and $c = 0, \cdots, p-1$, the uth user's DD grid for uplink[1] transmission will have

$$\begin{aligned} x_u[k,l] &= x_u[k' + d(N/q), l' + c(M/p)] \\ &= x_u[k',l']e^{j2\pi\left(c\frac{(u)_p}{p} - d\frac{\lfloor u/p \rfloor}{q}\right)}, \end{aligned} \tag{3}$$

where $(.)_p$ denotes modulo-p operation, $x_u[k',l'] \in \mathbb{A}$, where $\mathbb{A}$ denotes the modulation alphabet (e.g., QAM/PSK), and $x_u[k',l']$s denote the MN/K_u independent information symbols from uth user forming a $\frac{N}{q} \times \frac{M}{p}$ grid which is repeated (with a multiplicative phase) p times along the delay axis and q times along the Doppler axis, thereby spanning the entire $N \times M$ DD grid.

The delay-Doppler symbols of the uth user (i.e., $x_u[k,l]$s) are transformed to the TF domain using the inverse symplectic finite Fourier transform (ISFFT) and transmit windowing. Assuming rectangular windowing, the TF signal corresponding to the uth user is given by

$$X_u[n,m] = \frac{1}{\sqrt{MN}} \sum_{k=0}^{N-1} \sum_{l=0}^{M-1} x_u[k,l] e^{j2\pi\left(\frac{nk}{N} - \frac{ml}{M}\right)}. \tag{4}$$

Substituting (3) in (4), the corresponding TF signal of uth user is given by

---

[1]This scheme can be even applied for downlink transmission wherein the DD symbols intended for every user following (3) are superimposed together on the $N \times M$ DD grid and transmitted using OTFS modulation.
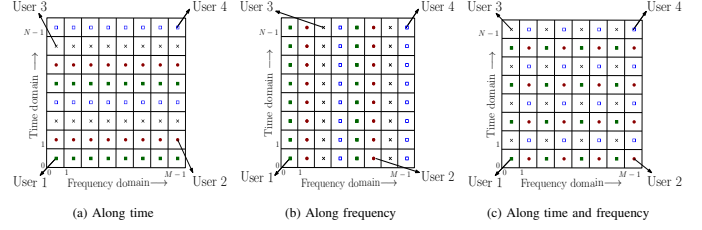

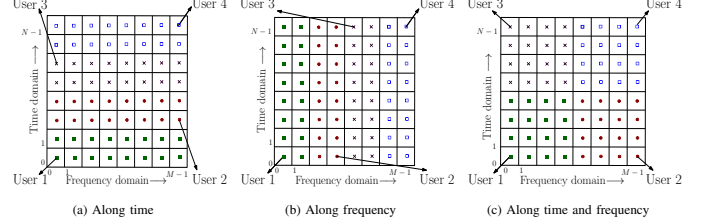Fig. 1: Multiplexing four users on an 8×8 TF grid according to the proposed ITFMA.

Fig. 2: Multiplexing four users on an 8×8 TF grid according to CTFMA in [13].

$$\begin{aligned} X_u[n,m] &= \frac{1}{\sqrt{MN}} \sum_{k'=0}^{\frac{N}{q}-1} \sum_{l'=0}^{\frac{M}{p}-1} \sum_{c=0}^{p-1} \sum_{d=0}^{q-1} x_u[k',l'] \\ &\quad e^{j2\pi\left(c\frac{(u)_p}{p} - d\frac{\lfloor u/p \rfloor}{q}\right)} e^{j2\pi\left(\frac{nk}{N} - \frac{ml}{M}\right)} \\ &= \frac{1}{\sqrt{MN}} \sum_{k'=0}^{\frac{N}{q}-1} \sum_{l'=0}^{\frac{M}{p}-1} x_u[k',l'] e^{j2\pi\left(\frac{nk'}{N} - \frac{ml'}{M}\right)} \\ &\quad \sum_{c=0}^{p-1} e^{j2\pi\frac{c}{p}((u)_p - m)} \sum_{d=0}^{q-1} e^{j2\pi\frac{d}{q}(\lfloor u/p \rfloor - n)}. \end{aligned} \tag{5}$$

Further simplifying (5), we get

$$X_u[n,m] = \frac{pq}{\sqrt{MN}} \sum_{k'=0}^{\frac{N}{q}-1} \sum_{l'=0}^{\frac{M}{p}-1} x_u[k',l'] e^{j2\pi\left(\frac{nk'}{N} - \frac{ml'}{M}\right)} \tag{6}$$

if $(m - (u)_p)_p = 0$ & $(n - \lfloor u/p \rfloor)_q = 0$, and zero otherwise. Note that the uth user's TF signal X_u occupies only few unique locations/resource bins (non-overlapping with other users' TF signals) on the TF grid which are spaced p bins apart along frequency and q bins along time. This allocation ensures that all the users' TF signals when put together cover the entire TF grid in a non-overlapping and interleaved way. Illustrating examples of allocation in the proposed ITFMA scheme are shown in Fig. 1, where an $N \times M = 8 \times 8$ TF grid gets allocated to four users. In contrast, the processing proposed in [13] results in contiguous allocation as illustrated in Fig. 2.

The TF signal $X_u[n,m]$ in (6) is converted into a time domain signal for transmission using Heisenberg transform with a transmit pulse denoted by $g_{tx}(t)$. The transmitted time domain signal of the uth user $x_u(t)$ is then given by

$$x_u(t) = \sum_{n=0}^{N-1} \sum_{m=0}^{M-1} X_u[n,m] g_{tx}(t - nT) e^{j2\pi m\Delta f(t-nT)}. \tag{7}$$

The signal $x_u(t)$ is transmitted through the uth user's channel whose complex baseband delay-Doppler channel response is

denoted by $h_u(\tau, \nu)$. At the BS, the received time domain signal $y(t)$ is given by

$$y(t) = \sum_{u=0}^{K_u-1} \int_\nu \int_\tau h_u(\tau,\nu)x_u(t-\tau)e^{j2\pi\nu(t-\tau)}\mathrm{d}\tau\mathrm{d}\nu + v(t), \tag{8}$$

where $v(t)$ denotes the additive white Gaussian noise at the BS receiver. The received signal at the BS is matched filtered with a receive pulse $g_{rx}(t)$, yielding the cross-ambiguity function $A_{g_{rx},y}(t,f)$ given by

$$A_{g_{rx},y}(t,f) = \int g_{rx}^*(t'-t)y(t')e^{-j2\pi f(t'-t)}\mathrm{d}t'. \tag{9}$$

The pulses $g_{tx}(t)$ and $g_{rx}(t)$ are chosen to be biorthogonal. Sampling $A_{g_{rx},y}(t,f)$ on the lattice Λ gives the matched filter output as

$$Y[n,m] = A_{g_{rx},y}(t,f)|_{t=nT,f=m\Delta f}. \tag{10}$$

When TF signal $Y[n,m]$ is received, if $h_u(\tau,\nu)$ has finite support bounded by $(\tau_{\max}, \nu_{\max})$ and if $A_{g_{rx}g_{tx}}(t,f) = 0$ for $t \in (nT - \tau_{\max}, nT + \tau_{\max})$, $f \in (m\Delta f - \nu_{\max}, m\Delta f + \nu_{\max})$, $\forall (n,m) \neq (0,0)$, then the BS can separate out the TF signal corresponding to each user $Y_u[n,m]$ as

$$Y_u[n,m] = Y[n,m] = H_u[n,m]X_u[n,m] + V[n,m] \tag{11}$$

if $(m - (u)_p)_p = 0$ & $(n - \lfloor u/p \rfloor)_q = 0$, and zero otherwise. Note that $V[n,m] \sim \mathcal{CN}(0,(pq)^2)$ to compensate for the power boost up in (6) due to quasi-periodic repetition of symbols in the DD domain. Finally, $Y_u[n,m]$ can be mapped individually to the DD plane as $y_u[k,l]$ for every u using SFFT transform as

$$y_u[k,l] = \frac{1}{\sqrt{MN}} \sum_{k=0}^{N-1}\sum_{l=0}^{M-1} Y_u[n,m]e^{-j2\pi\left(\frac{nk}{N} - \frac{ml}{M}\right)}. \tag{12}$$

For detecting the uth user's MN/K_u information symbols $x_u[k',l']$, the sufficient observables are $y_u[k'',l'']$ for $k'' = 0, \cdots, \frac{N}{q}-1$, $l'' = 0, \cdots, \frac{M}{p}-1$, and the input-output relation can be derived as given by (13) by substituting (3) in the general input-output relation derived in [5], where $v_u[k'',l'']$ denotes the additive white Gaussian noise corresponding to the uth user and $\tilde{h}_u(k,l)$ is the sampled version of the function $\tilde{h}_u(\nu,\tau)$ which is obtained as the circular convolution of $h_u(\tau,\nu)$ with the window function at $\nu = \frac{k}{NT}$ and $\tau = \frac{l}{M\Delta f}$ [2],[5]. Vectorizing (13), we get

$$\mathbf{y}'_u = \mathbf{H}'_u\mathbf{x}'_u + \mathbf{v}'_u, \tag{14}$$

where $\mathbf{x}'_u \in \mathbb{C}^{MN/K_u \times 1}$, $\mathbf{x}'_u(k' + Nl'/q) = x_u[k',l']$, and $\mathbf{H}'_u \in \mathbb{C}^{MN/K_u \times MN/K_u}$. This allows MUI-free reception for every user in the TF domain and subsequent detection in the DD domain.

III. PAPR OF THE PROPOSED SCHEME

In this section, we analyze the PAPR of the proposed uplink ITFMA scheme. Low PAPR is highly desired in cellular uplink transmissions where the transmitters are low cost hand-held devices. As discussed in Sec. II, for uplink transmission, each user places the information symbols on the delay-Doppler grid as per (3) and then does an OTFS transform (ISFFT) which converts these symbols to the TF domain. A multicarrier modulation technique (assume OFDM, i.e., $g_{tx}(t)$ being a rectangular pulse) takes the TF signal to time domain for transmission. PAPR of this time-domain signal has to be analyzed. It has been shown in [16] that for any user u, the discrete time samples (assuming Nyquist sampling) of this time domain signal corresponding to one OTFS transmit frame are nothing but the vectorized and scaled version of the N-point IDFT (along the Doppler domain) values of the data symbols $x_u[k,l]$. Hence the PAPR of discrete time samples corresponding to one transmit OTFS frame from an uplink user depends on the way the Doppler bins are populated by the user. By the proposed scheme, every user occupies all the N Doppler bins with N/q independent entries quasi-periodically repeated q times and all the M delay bins with M/p independent entries quasi-periodically repeated p times. Hence the maximum PAPR of the discrete time signal of a user, denoted by $\text{PAPR}_{\max}$, can be as high as N assuming MPSK (for some user $u = 0$, IDFT operations can result in all N symbols adding coherently) and does not depend on either the number of delay bins M [16] or the number of users K_u.

A. CCDF of PAPR

It is also important to consider the complementary cumulative distribution function (CCDF) of PAPR. Towards this, we compute the nth ($n = 0, \cdots, N-1$) N-point IDFT of $x_u[k,l]$, $k = 0, \cdots, N-1$, for a given l, as

$$\sum_{k=0}^{N-1} x_u[k,l]e^{\frac{j2\pi nk}{N}} = \begin{cases} q\sum_{k'=0}^{N/q-1} x_u[k',l]e^{\frac{j2\pi nk'}{N}} & \text{if } (n - \lfloor u/p \rfloor)_q = 0 \\ 0 & \text{otherwise.} \end{cases} \tag{15}$$

The non-zero samples in (15) are in fact $\frac{N}{q}$-point IDFT values of $x_u[k',l]e^{\frac{j2\pi\lfloor u/p \rfloor k'}{N}}$, $k' = 0, \cdots, \frac{N}{q} - 1$ for a given delay index l and each of them follows a complex Gaussian distribution with zero mean if N/q is large (by central limit theorem). Hence the power of these samples are exponential distributed with mean q times the average power of one frame. Therefore the CCDF of PAPR which is the probability that PAPR of the transmit samples is greater than a threshold γ ($\gamma \leq \text{PAPR}_{\max}$) is given by

$$P(\text{PAPR} > \gamma) = 1 - P(\text{PAPR} \leq \gamma)$$
$$\approx 1 - \prod_{i=0}^{\frac{M}{p}-1}\prod_{j=0}^{\frac{N}{q}-1}\left(1 - e^{\gamma/q}\right)$$
$$= 1 - \left(1 - e^{\gamma/q}\right)^{MN/K_u}. \tag{16}$$

B. DFT spread ITFMA

DFT based precoding can help in reducing PAPR. In DFT spread ITFMA (DFT-s-ITFMA), an $\frac{N}{q}$-point DFT is applied on the information symbols $x_u[k',l]$, $k' = 0, \cdots, \frac{N}{q} - 1$, for each l before applying ISFFT operation on the delay-Doppler

$$y_u[k'', l''] = \sum_{k=0}^{N-1} \sum_{l=0}^{M-1} x_u[k,l]\tilde{h}_u[(k''-k)_N, (l''-l)_M] + v_u[k'', l'']$$

$$= \sum_{k'=0}^{\frac{N}{q}-1} \sum_{l'=0}^{\frac{M}{p}-1} \sum_{c=0}^{p-1} \sum_{d=0}^{q-1} x_u[k',l']e^{j2\pi\left(c\frac{(u)_p}{p} - d\frac{\lfloor u/p \rfloor}{q}\right)}\tilde{h}_u[(k'' - (k' + d(N/q)))_N, (l'' - (l' + c(M/p)))_M] + v_u[k'', l'']$$

$$= \sum_{k'=0}^{\frac{N}{q}-1} \sum_{l'=0}^{\frac{M}{p}-1} x_u[k',l'] \sum_{c=0}^{p-1} \sum_{d=0}^{q-1} e^{j2\pi\left(c\frac{(u)_p}{p} - d\frac{\lfloor u/p \rfloor}{q}\right)}\tilde{h}_u[(k'' - d(N/q) - k')_N, (l'' - c(M/p) - l')_M] + v_u[k'', l''].$$

$$(13)$$

symbols $x_u[k,l]$. This will bring down the PAPR$_{\text{max}}$ of each user. For example, for user $u = 0$, PAPR$_{\text{max}}$ comes down to q times the PAPR of constellation $\mathbb{A}$.

IV. RESULTS AND DISCUSSIONS

In this section, we present the BER performance of the proposed scheme under maximum likelihood (ML) detection for small dimension systems and minimum mean square error (MMSE) detection for large dimension systems and compare with the performance of the CTFMA scheme presented in [13]. Figure 3 shows the BER performance of both of these TF multiplexing schemes for $i)$ $K_u = 2$ ($p = 1, q = 2$; $g_1 = 1, g_2 = 2$), $ii)$ $K_u = 4$ ($p = q = 2$; $g_1 = g_2 = 2$), and $iii)$ $K_u = 8$ ($p = 4, q = 2$; $g_1 = 4, g_2 = 2$) with $M = N = 4$ using ML detection[2]. Figure 4 shows the BER performance for $i)$ $K_u = 8$ ($p = 4, q = 2$; $g_1 = 4, g_2 = 2$) and $ii)$ $K_u = 16$ ($p = 8, q = 2$; $g_1 = 8, g_2 = 2$) with $M = 32, N = 8$ using MMSE detection. For both figures, a carrier frequency of 4 GHz, subcarrier spacing of 15 kHz, and BPSK modulation are used. A 4-tap delay-Doppler channel with a delay profile of $\{0, 16.66, 33.33, 50\}$ μs and a 10-tap channel with a delay profile of $\{0, 2.08, 4.16, 6.25, 8.33, 10.42, 12.5, 14.58, 16.66, 18.75\}$ μs are used in Figs. 3 and 4, respectively. Also, exponential power delay profile and Jakes Doppler spectrum [17] for all the users are used. The Doppler shift corresponding to the jth tap of uth user is generated using $\nu_{u,j} = \nu_{\text{max}} \cos(\theta_{u,j})$, where for all the users ν_{max} is taken to be 1 KHz in Fig. 3 and 1.875 KHz in Fig. 4, and $\theta_{u,j}$ is uniformly distributed over $[-\pi, \pi]$. From both the figures, we observe that the proposed ITFMA outperforms CTFMA in all cases (e.g., in Fig. 3, ITFMA with 4 users has about 3 dB SNR advantage compared to CTFMA at 10^{-3} BER). The reason for this better performance can be explained as follows. In the CTFMA scheme, the signal of each user is restricted to only a contiguous or a localized region on the TF plane and employs a reduced point SFFT to detect the received TF signal, due to which the signal may experience correlated TF fading depending on the channel's coherence bandwidth, coherence time, and the localized region allotted to the user (specified by the choice of g_1 and g_2). This limits the resulting performance. Whereas, ITFMA assigns TFRBs to each user in such a way that the resource blocks of the users are well distributed in the TF grid, thereby offering the potential for better performance.

[2]The parameters g_1 and g_2 represent the interleaving intervals in the delay axis and the Doppler axis, respectively, in [13].
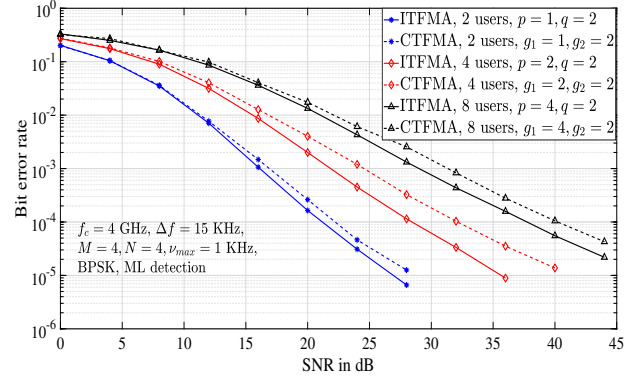

Fig. 3: BER performance comparison between ITFMA and CTFMA with $M = N = 4$, $K_u = 2, 4, 8$ under ML detection.
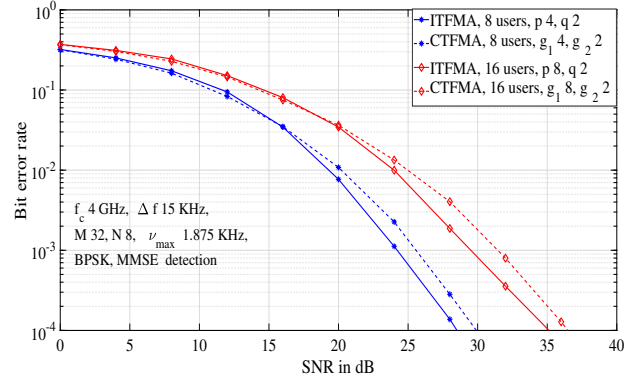

Fig. 4: BER performance comparison between ITFMA and CTFMA with $M = 32, N = 8, K_u = 8, 16$ under MMSE detection.

In Fig. 5, we plot the analytical and simulated CCDFs of the discrete-time PAPR (Nyquist sampled) of a user using ITFMA scheme with four users, 4-QAM, and the following parameters: $p = 4, q = 1$ (frequency interleaved), $p = 1, q = 4$ (time interleaved), and $p = 2, q = 2$ (time-frequency interleaved) for two systems with $i)$ $M = 128, N = 64$ and $ii)$ $M = 128, N = 128$. Observe that the simulated CCDFs match closely with analytical CCDFs for higher values of N/q. Also, the CCDF curves shift to the right with increase in the parameter q. This is because interleaving users along time produces $(q-1)N/q$ zeros in time domain (15) and increases the chance of getting large peaks. Hence the method of interleaving users in frequency alone (by choosing parameter q as one) gives the lowest CCDF.
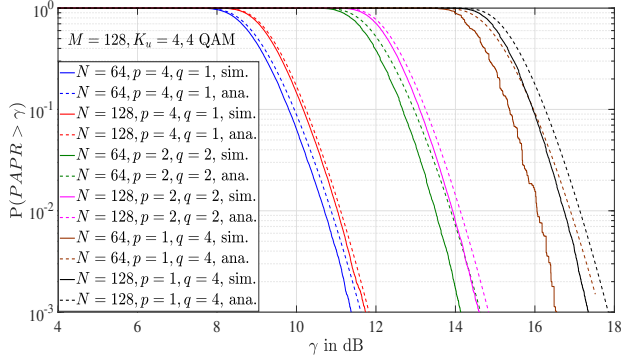
Fig. 5: Analytical and simulated CCDFs of PAPR of ITFMA.
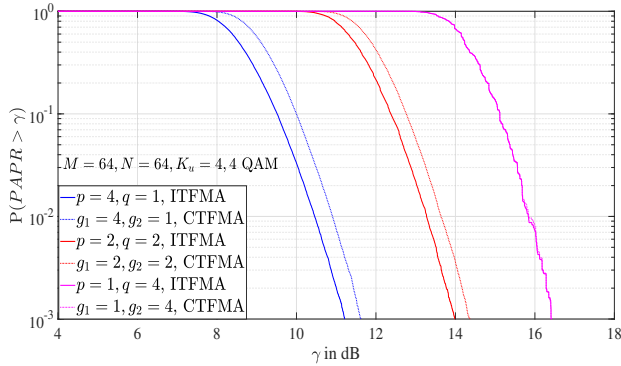

Fig. 6: Comparison between simulated CCDFs of PAPR of ITFMA and CTFMA for 4-QAM and $M = N = 64$.

Figure 6 compares the simulated CCDFs of discrete-time PAPR of ITFMA and CTFMA with four users, 4-QAM, and the following parameters: $(p = 4, q = 1; g_1 = 4, g_2 = 1)$, $(p = q = 2; g_1 = g_2 = 2)$, and $(p = 1, q = 4; g_1 = 1, g_2 = 4)$ for $M = 64, N = 64$. It can be seen that ITFMA has a better PAPR characteristics compared to CTFMA for all cases except for $(p = 1, q = 4; g_1 = 1, g_2 = 4)$, i.e., multiplexing users only along time, where both show almost same PAPR characteristics.

Figure 7 shows the simulated CCDFs of discrete time PAPR (Nyquist sampled) of DFT-s-ITFMA and ITFMA with $K_u = 4$, $\{(p = 4, q = 1), (p = q = 2), (p = 1, q = 4)\}$, 16-QAM, and $M = N = 64$. The simulated CCDFs of CTFMA and DFT-s-CTFMA (wherein $\frac{N}{g_2}$-point DFT is applied as precoding on the delay-Doppler symbols before placing them along Doppler axis at regular intervals of g_2 bins apart [13] and applying ISFFT) with parameters $\{(g_1 = 4, g_2 = 1), (g_1 = g_2 = 2), (g_1 = 1, g_2 = 4)\}$ are also plotted for comparison. Observe that the CCDF of DFT-s-ITFMA is better than those of other schemes. For example, with $(p = 4, q = 1)$, the PAPR of DFT-s-ITFMA is almost 8.5 dB lower than that of ITFMA at a probability of 10^{-3}. Also, note that DFT precoding can have an impact on the BER performance of the respective multiplexing schemes as it can overrule partially the effect of spreading of symbols along the time domain attained by OTFS transform.
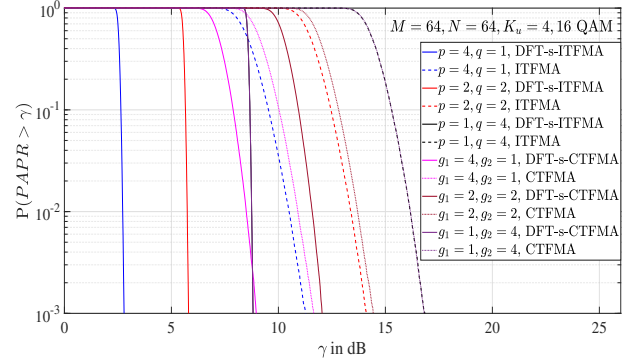

Fig. 7: Comparison between simulated CCDFs of PAPR of ITFMA, DFT-s-ITFMA, CTFMA, and DFT-s-CTFMA for 16-QAM and $M = N = 64$.

V. CONCLUSIONS

We proposed a novel TF interleaved multiple access scheme using OTFS on the uplink. This scheme was found to achieve better performance compared to the scheme presented in [13], where the signal of each user is restricted to only a contiguous or a localized region on the TF plane and the resulting correlated nature of the TF fading limited the achieved performance. In the proposed scheme, on the other hand, TFRBs are assigned to each user in such a way that users' resource blocks are well distributed in the TF grid thereby offering the potential for better performance. We also investigated the PAPR of the proposed scheme by characterizing its CCDF analytically and illustrated its good PAPR performance.

REFERENCES

[1] W. C. Jakes, *Microwave Mobile Communications*, New York: IEEE Press, reprinted, 1994.

[2] R. Hadani, S. Rakib, M. Tsatsanis, A. Monk, A. J. Goldsmith, A. F. Molisch, and R. Calderbank, "Orthogonal time frequency space modulation," in *Proc. IEEE WCNC'2017*, Mar. 2017, pp. 1-7.

[3] R. Hadani, S. Rakib, S. Kons, M. Tsatsanis, A. Monk, C. Ibars, J. Delfeld, Y. Hebron, A. J. Goldsmith, A. F. Molisch, and R. Calderbank, "Orthogonal time frequency space modulation," online: arXiv:1808.00519v1 [cs.IT] 1 Aug 2018.

[4] L. Li, H. Wei, Y. Huang, Y. Yao, W. Ling, G. Chen, P. Li, and Y. Cai, "A simple two-stage equalizer with simplified orthogonal time frequency space modulation over rapidly time-varying channels," online: arXiv:1709.02505v1 [cs.IT] 8 Sep 2017.

[5] P. Raviteja, K. T. Phan, Y. Hong, and E. Viterbo, "Interference cancellation and iterative detection for orthogonal time frequency space modulation," *IEEE Trans. Wireless Commun.*, vol. 17, no. 10, pp. 6501-6515, Aug. 2018.

[6] K. R. Murali and A. Chockalingam, "On OTFS modulation for high-Doppler fading channels," *Proc. ITA'2018*, Feb. 2018.

[7] A. Farhang, A. R. Reyhani, L. E. Doyle, and B. Farhang-Boroujeny, "Low complexity modem structure for OFDM-based orthogonal time frequency space modulation," *IEEE Wireless Commun. Lett.*, doi: 10.1109/LWC.2017.2776942.

[8] G. D. Surabhi, R. M. Augustine, and A. Chockalingam, "On the diversity of uncoded OTFS modulation in doubly-dispersive channels," *IEEE Trans. Wireless Commun.*, vol. 18, no. 6, pp. 3049-3063, Jun. 2019.

[9] P. Raviteja, Y. Hong, E. Viterbo, and E. Biglieri, "Practical pulse shaping waveforms for reduced-cyclic-prefix OTFS," *IEEE Trans. Veh Tech.*, doi: 10.1109/TVT.2018.2878891.

[10] P. Raviteja, K. T. Phan, and Y. Hong, "Embedded pilot-aided channel estimation for OTFS in delay-Doppler channels," online: arXiv:1808.08360 [cs.IT] 25 Aug 2018.

[11] M. K. Ramachandran and A. Chockalingam, "MIMO-OTFS in high-Doppler fading channels: signal detection and channel estimation," *Proc. IEEE GLOBECOM'2018*, pp. 206-212, Dec. 2018.

[12] S. Rakib and R. Hadani, "Multiple access in wireless telecommunications system for high-mobility applications," *US Patent No. US9722741B1*, Aug. 2017.

[13] V. Khammammetti and S. K. Mohammed, "OTFS based multiple-access in high Doppler and delay spread wireless channels," *IEEE Wireless Commun. Lett.*, doi: 10.1109/LWC.2018.2878740.

[14] G. D. Surabhi, R. M. Augustine, and A. Chockalingam, "Multiple access in the delay-Doppler domain using OTFS modulation," online: arXiv:1902.03415 [sc.IT] 9 Feb 2019.

[15] Z. Ding, R. Schober, P. Fan, and H. V. Poor, "OTFS-NOMA: an efficient approach for exploiting heterogeneous user mobility profiles," online: arXiv:1904.02783 [sc.IT] 4 Apr 2019.

[16] G. D. Surabhi, R. M. Augustine, and A. Chockalingam, "Peak-to-average power ratio of OTFS modulation," *IEEE Commun. Lett.*, vol. 23, no. 6, pp. 999-1002, Jun. 2019.

[17] F. Hlawatsch and G. Mats, *Wireless Communications over Rapidly Time-Varying Channels*, Academic Press, 2011.